Scientific Research Publishing

World Journal of Engineering and Technology, 2017, 5, 27-41
http://www.scirp.org/journal/wjet
ISSN Online: 2331-4249
ISSN Print: 2331-4222

Analytical Identification of Magnetic Faults Induced by Material Properties and Mechanical Tolerance in PM Synchronous Motor

Yinquan Yu*, Quan Jiang, Nay Lin Htun Aung

Drive Systems and Technologies Division, Data Storage Institute, A-Star, Singapore
Email: *yu_yinquan@dsi.a-star.edu.sg

How to cite this paper: Yu, Y.Q., Jiang, Q. and Aung, N.L.H. (2017) Analytical Identification of Magnetic Faults Induced by Material Properties and Mechanical Tolerance in PM Synchronous Motor. *World Journal of Engineering and Technology*, **5**, 27-41.
https://doi.org/10.4236/wjet.2017.51004

Received: October 12, 2016
Accepted: February 17, 2017
Published: February 20, 2017

Abstract

This paper presents an analytical model suitable for analyzing Permanent Magnet Synchronous motors. The difference between mass eccentricity and magnet eccentricity is described. The full derived vibration mathematical model incorporates both the electrical domain and mechanical domain. The shaft bending force, mass eccentricity exciting force, aerodynamic exciting force, and unbalanced-Magnet-Pull (UMP) are introduced in this three-dimensional motor model. The relative displacement between rotor and stator is calculated in order to avoid rotor to stator rub. The experiments were conducted with Laser Vibrometer for verifying the analysis results. The measurement results prove the effectiveness of the proposed analytic method.

Keywords

Mass Eccentricity, Magnet Eccentricity, Unbalanced-Magnet-Pull (UMP), Vibration, Laser Vibrometer

1. Introduction

Because many tools and machines used today are derived by motors, vibrations can be devastating. Vibration shortens the life of the motor and damages all the components around them. In order to fully understand motor vibration behavior, a thorough theoretical derivation of motor dynamics should be carried out as they can disclose clearly the global performance of the motor. Generally, four types of excitation force such as mass eccentricity force, shaft bending force, UMP force, and fan aerodynamic force can generate the motor lateral and axial vibration and produce motor noise. Mechanical unbalance in a rotating machine is a condition of unequal mass distribution at each section of the rotor [1]. When the unbalanced machine is rotating, the rotor mass center does not coin-

cide with the rotating axis and the eccentric force is generated on the rotor. Vibration and stress are induced in the rotor itself and in its supporting structure, which may gradually lead to excessive wear in the joints: bearings, bushings, shafts and spindles. Eventually, the whole system may be broken down. This is a very common malfunction in rotating machines. Vibrations due to one machine's mechanical unbalance may also be transmitted through the floor to adjacent machinery and seriously impair its accuracy or proper functioning, or be transmitted through either the machine structure or the air to generate structure bone or air bone acoustic noise, which will decrease the machine's performance and the quality of the working environment.

Several researchers have studied rotor mass eccentricity in rotating machines in recent years. Rajagopalan *et al*. [2] proposed a methodology to distinguish mechanically unbalanced rotors by monitoring signals at two side bands of the fundamental frequency of the Brushless DC (BLDC) motor phase current under no stationary conditions. Huang [3] studied the characteristics of torsion vibrations of an unbalanced shaft using the numerical simulation method, and the simulation results are agreeable with the experimental results. Concari *et al*. [4] proposed a method to discern mechanical torque unbalance in the induction motor. Their method uses the motor phase current sideband component to estimate the unbalance. Kr. Jalan and Mohanty [5] used a motor-based fault diagnosis technology to diagnose the misalignment or unbalanced motor by building the methodical model and calculating residual vibration on the healthy motor.

Other than Mechanical Unbalance (MU), Unbalance Magnetic Pull (UMP) is another big concern that demands a thorough study and understanding of motor design and diagnosis. In fact, UMP generated by rotor eccentricity faults has been an active research topic for more than a hundred years [6]. A switched reluctance motor by Garrigan *et al*. [7] considered only static rotor eccentricity faults, but also dynamic rotor eccentricity faults. The authors show that UMP can be quickly predicted by their developed Magnetic Equivalent Circuit (MEC) approach when the relative rotor eccentricity is less than 25% of the normal air-gap. Based on the motor shaft movement orbit from a mechanical point of view, Werner [8] uses shaft vibration signals to study induction motor static UMP due to the static eccentricity fault. On the other hand, Rajagopalan *et al*. [9] use a field reconstruction method to study static UMP in a Permanent Magnet Synchronous Motor (PMSM) Bi *et al*. [10] analyzed and calculated dynamic UMP within one motor revolution. The lowest order of the extrinsic UMP harmonic is one-in-one motor revolution. Even though there is no eccentricity distance between the rotor center and stator center, the UMP is only related to EM structures such as the Pole pair number, and the slot number still exists. This type of UMP is called intrinsic UMP, which is formed in even harmonics and can be eliminated by an even slot number. In this paper, the BLDC mathematic model has introduced and validated by oriental motor experimental case study.

2. Mathematical Model

Due to machining and assemble accuracy limitations, an electrical motor could have a few types of eccentricities. The most important eccentricities in a motor are rotor mass eccentricities, magnetic eccentricities, and rotor bending deflection. In this work, we consider a horizontal mounting motor for analysis. Its dynamic model can be illustrated as in Figure 1. The PM synchronous motor model consists of two lumping mass: rotor mass, Mr, and stator mass, Ms. The rotor is supported by an oil film sleeve bearing at the two ends of the shaft. The oil film sleeve bearing can be modeled by stiffness and damping matrix. For a rotating electrical machine, an additional magnetic stiffness matrix Cn between the rotor and stator exists, which describes the electromagnetic coupling between them. Due to the sleeve bearing housing, damping effect is very low compared to its oil film. Therefore, the bearing house stiffness matrix is the only one to be considered. The motor normally is mounted on the soft base to isolate the vibration from the ground. Compared to the stator of a PM synchronous motor, the mounting media is more flexible, so stiffness and damping matrix is taken into account.

In order to simplify the analysis, the dynamic model can be separated into three sub-models: rotor model, bearing housing model, and stator model. Rotor model includes magnet, rotor yoke, and shaft; bearing house model includes bearing components; stator model includes armature winding, stator core, motor base, left-side and right bearing covers.

2.1. Rotor Model

Figure 2 shows all forces are applied on rotor. they include rotor mass unbalance force, oil film of bearing reaction forces, magnetic unblance forces in *x*, *y*, *z* directions and can be present as:

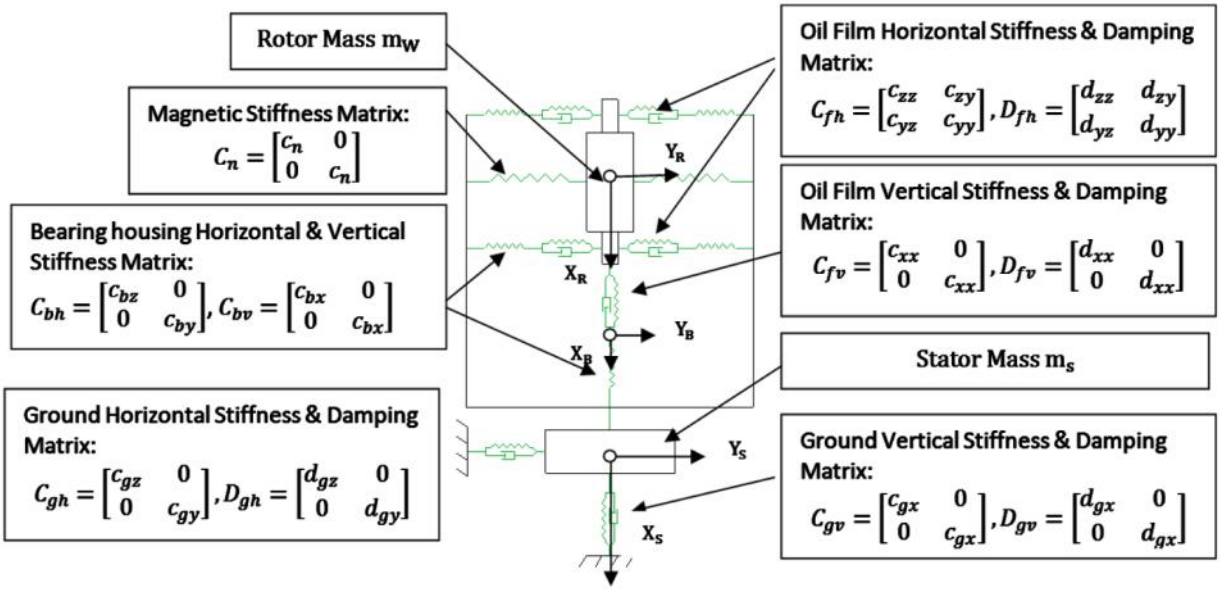

Figure 1. Dynamic model of PM synchronous motor.

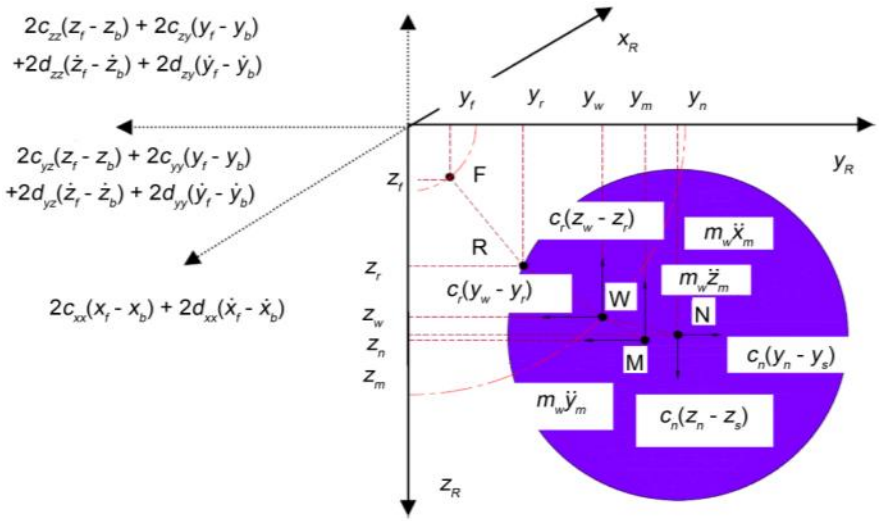

Figure 2. Dynamic force on rotor of PM synchronous motor.

$$F_{X-R} = m_w\ddot{x}_m - 2d_{xx}\left(\dot{x}_f - \dot{x}_b\right) - 2c_{xx}\left(x_f - x_b\right), \tag{1}$$

$$\begin{aligned} F_{Y-R} = {} & c_n\left(y_n - y_s\right) - m_w\ddot{y}_m - c_r\left(y_w - y_r\right) - 2c_{yz}\left(z_f - z_b\right) \\ & - 2c_{yy}\left(y_f - y_b\right) - 2d_{yz}\left(\dot{z}_f - \dot{z}_b\right) - 2d_{yy}\left(\dot{y}_f - \dot{y}_b\right), \end{aligned} \tag{2}$$

$$\begin{aligned} F_{Z-R} = {} & c_n\left(z_n - z_s\right) - m_w\ddot{z}_m - c_r\left(z_w - z_r\right) - 2c_{zz}\left(z_f - z_b\right) \\ & - 2c_{zy}\left(y_f - y_b\right) - 2d_{zz}\left(\dot{z}_f - \dot{z}_b\right) - 2d_{zy}\left(\dot{y}_f - \dot{y}_b\right), \end{aligned} \tag{3}$$

where m_w is rotor mass. c_{xx}, c_{yy}, c_{zz} is the bearing stiffness coefficient in X, Y and Z directions; d_{xx}, d_{yy}, d_{zz} is the bearing damping coefficient in X, Y and Z directions.

2.2. Bearing Housing Model

Figure 3 shows all forces on the bearing. Since the mass of bearing housing is quite small compared to the mass of stator $m_{\text{bearing}}\ddot{x}_b$, $m_{\text{bearing}}\ddot{y}_b$, $m_{\text{bearing}}\ddot{z}_b$ and can be ignored, the dynamic action force on the X_B, Y_B, Z_B is only oil film action force and stator action force and is:

$$F_{X-B} = c_{bx}\left(x_b - x_s\right) - c_{xx}\left(y_f - y_b\right) - d_{xx}\left(\dot{y}_f - \dot{y}_b\right), \tag{4}$$

$$\begin{aligned} F_{Y-B} = {} & c_{yz}\left(z_f - z_b\right) + c_{yy}\left(y_f - y_b\right) + d_{yz}\left(\dot{z}_f - \dot{z}_b\right) \\ & + d_{yy}\left(\dot{y}_f - \dot{y}_b\right) - c_{by}\left(y_b - y_s\right), \end{aligned} \tag{5}$$

$$\begin{aligned} F_{Z-B} = {} & c_{zz}\left(z_f - z_b\right) + c_{zy}\left(y_f - y_b\right) + d_{zz}\left(\dot{z}_f - \dot{z}_b\right) \\ & + d_{zy}\left(\dot{y}_f - \dot{y}_b\right) - c_{bz}\left(z_b - z_s\right). \end{aligned} \tag{6}$$

2.3. Stator Model

It is assumed that the motor is flexibly mounted on the ground through horizontal and vertical spring with damper. The spring stiffness and damper coefficient in X and Y direction are same. The stator mass is located at its geometry

center. The dynamic action forces on the X_S, Y_S, Z_S is two end bearing house action forces, rotor magnet action force and supporting spring and damper action forces. In Figure 4, the individual forces on the stator in X, Y and Z directions are:

$$F_{X-S} = m_s\ddot{x}_s - d_{gx}\dot{x}_s - \left(c_{gx} + c_{bx}\right)x_s + c_{bx}x_b, \tag{7}$$

$$\begin{aligned} F_{Y-R} = {} & c_n\left(y_n - y_s\right) - m_w\ddot{y}_m - c_r\left(y_w - y_r\right) - 2c_{yz}\left(z_f - z_b\right) \\ & - 2c_{yy}\left(y_f - y_b\right) - 2d_{yz}\left(\dot{z}_f - \dot{z}_b\right) - 2d_{yy}\left(\dot{y}_f - \dot{y}_b\right), \end{aligned} \tag{8}$$

$$\begin{aligned} F_{Z-R} = {} & c_n\left(z_n - z_s\right) - m_w\ddot{z}_m - c_r\left(z_w - z_r\right) - 2c_{zz}\left(z_f - z_b\right) \\ & - 2c_{zy}\left(y_f - y_b\right) - 2d_{zz}\left(\dot{z}_f - \dot{z}_b\right) - 2d_{zy}\left(\dot{y}_f - \dot{y}_b\right), \end{aligned} \tag{9}$$

The following assumptions are made for the geometrical relationship of the

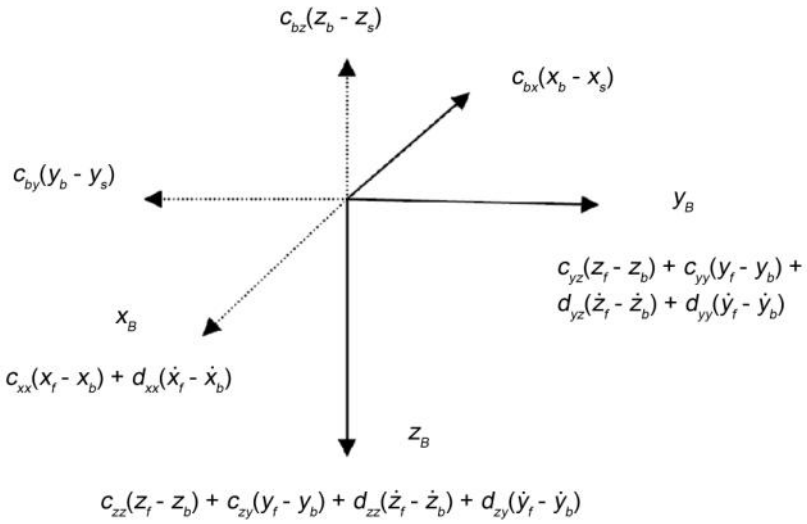

Figure 3. Dynamic force on the bearing housing of the PM synchronous motor.

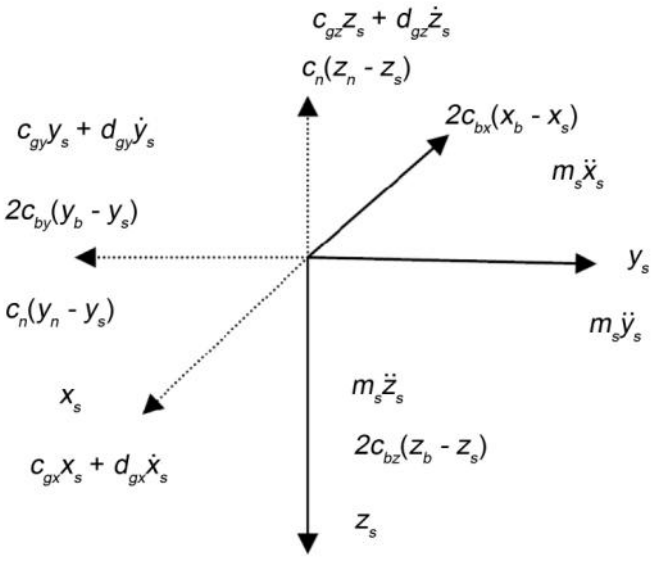

Figure 4. Dynamic force on the stator of the PM synchronous motor.

rotor mass magnet system:

- The distance between fluid bearing orbit and pre-bent shaft orbit is $\hat{e}_r$;
- The distance between rotor orbit and rotor mass center is $\hat{e}_m$;
- The distance between rotor orbit and rotor magnet center is $\hat{e}_n$.

Thus from Figure 2 the equations can be derived as:

$$z_r = z_f + \hat{e}_r \cos\left(\omega t + \varphi_r\right), \tag{10}$$

$$y_r = y_f + \hat{e}_r \sin\left(\omega t + \varphi_r\right), \tag{11}$$

$$z_m = z_w + \hat{e}_m \cos\left(\omega t + \varphi_m\right), \tag{12}$$

$$y_m = y_w + \hat{e}_m \sin\left(\omega t + \varphi_m\right), \tag{13}$$

$$z_n = z_w + \hat{e}_n \cos\left(\omega t + \varphi_n\right), \tag{14}$$

$$y_n = y_w + \hat{e}_n \sin\left(\omega t + \varphi_n\right). \tag{15}$$

Given by motor whole system mass matrix $\boldsymbol{M}$, damping matrix $\boldsymbol{D}$, stiffness Matrix $\boldsymbol{C}$, coordinate vector and excitation force vector, the linear inhomogeneous differential equation can be derived:

$$\boldsymbol{M}\ddot{\boldsymbol{q}} + \boldsymbol{D}\dot{\boldsymbol{q}} + \boldsymbol{C}\boldsymbol{q} = \boldsymbol{f}. \tag{16}$$

$\boldsymbol{q}$ is coordinate vector and can be present as:

$$\boldsymbol{q} = \begin{bmatrix} z_s & y_s & x_s & z_w & y_w & x_w & z_f & y_f & x_f & z_b & y_b & x_b \end{bmatrix}^{\mathrm{T}}. \tag{17}$$

System mass matrix $\boldsymbol{M}$ can be expressed as:

$$\boldsymbol{M} = \begin{pmatrix} \boldsymbol{M}_{11} & 0 \\ 0 & 0 \end{pmatrix}, \tag{18}$$

and $\boldsymbol{M}_{11}$ is 6×6 mass matrix which includes mass of stator and that of rotor as:

$$\boldsymbol{M}_{11} = \begin{pmatrix} M_s & 0 & . & . & . & 0 \\ 0 & M_s & . & . & . & . \\ . & . & M_s & . & . & . \\ . & . & . & M_w & . & . \\ . & . & . & . & M_w & 0 \\ 0 & . & . & . & 0 & M_w \end{pmatrix}. \tag{19}$$

System damping matrix $\boldsymbol{D}$ also can be given by:

$$\boldsymbol{D} = \begin{pmatrix} \boldsymbol{D}_{11} & 0 \\ 0 & \boldsymbol{D}_{22} \end{pmatrix}, \tag{20}$$

and $\boldsymbol{D}_{11}$ is damping of oil film in bearing between stator and ground in *xyz* directions and as:

$$\boldsymbol{D}_{11} = \begin{pmatrix} -d_{gz} & 0 & . & . & . & 0 \\ 0 & -d_{gy} & . & . & . & . \\ . & . & -d_{gx} & . & . & . \\ . & . & . & 0 & . & . \\ . & . & . & . & 0 & . \\ 0 & . & . & . & . & 0 \end{pmatrix}, \tag{21}$$

$$\boldsymbol{D}_{22}=\begin{pmatrix} -2d_{zz} & -2d_{zy} & 0 & 2d_{zz} & 2d_{zy} & 0 \\ -2d_{yz} & -2d_{yy} & 0 & 2d_{yz} & 2d_{yy} & 0 \\ 0 & 0 & -2d_{xx} & . & . & . \\ -d_{zz} & -d_{zy} & 0 & d_{zz} & d_{zy} & . \\ d_{yz} & d_{yy} & . & d_{zy} & d_{yy} & . \\ 0 & . & . & . & . & 0 \end{pmatrix}. \tag{22}$$

$\boldsymbol{D}_{22}$ is damping of oil film in bearing between rotor and stator in *xyz* directions.

System stiffness matrix $\boldsymbol{C}$ also can be represented as:

$$\boldsymbol{C}=\begin{pmatrix} \boldsymbol{C}_{11} & \boldsymbol{C}_{12} \\ \boldsymbol{C}_{21} & \boldsymbol{C}_{22} \end{pmatrix}, \tag{23}$$

and it includes four sub matrix which are present as:

$$\boldsymbol{C}_{11}=\begin{pmatrix} c_n+2c_{bz}-c_{gz} & 0 & . & -c_n & . & 0 \\ 0 & 2c_{by}+c_n-c_{gy} & . & . & . & . \\ . & . & -c_{gx}-2c_{bx} & . & . & c_n \\ . & . & . & 0 & . & . \\ . & . & . & . & 0 & 0 \\ 0 & . & . & . & 0 & -2c_{zz} \end{pmatrix} \tag{24}$$

which C_n is the stiffness of rotor in radial direction respectively; C_{zz} is that of rotor in axial direction. C_{by} and C_{gy}, C_{bz} and C_{gz} are the stiffness of bearing and ground in *y* and *z* directions respectively.

$$\boldsymbol{C}_{12}=\begin{pmatrix} 0 & . & . & -2c_{bz} & . & 0 \\ . & . & . & . & -2c_{by} & . \\ . & . & . & . & . & 2c_{bx} \\ C_n & . & . & . & . & . \\ . & . & . & . & . & . \\ 0 & . & . & . & . & 0 \end{pmatrix}. \tag{25}$$

C_{bx} of C_{12} is the stiffness of bearing in *x* direction. Moreover, $\boldsymbol{C}_{12}=\boldsymbol{C}_{21}$.

$$\boldsymbol{C}_{22}=\begin{pmatrix} -2c_{zz} & -2c_{zy} & . & 2c_{zz} & 2c_{zy} & 0 \\ -2c_{yz} & -2c_{yy} & . & 2c_{yz} & 2c_{yy} & . \\ . & . & . & . & . & . \\ -c_{zz} & -c_{zy} & . & c_{zz} & c_{zy} & . \\ c_{yz} & c_{yy} & . & c_{zy} & c_{yy} & . \\ 0 & . & . & . & . & 0 \end{pmatrix}. \tag{26}$$

In $\boldsymbol{C}_{22}$ Matrix, C_{zy} is the stiffness of rotor in *z* direction when the force in *y* direction is applied.

$$\boldsymbol{C}_{22}=\begin{pmatrix} -2c_{zz} & -2c_{zy} & . & 2c_{zz} & 2c_{zy} & 0 \\ -2c_{yz} & -2c_{yy} & . & 2c_{yz} & 2c_{yy} & . \\ . & . & . & . & . & . \\ -c_{zz} & -c_{zy} & . & c_{zz} & c_{zy} & . \\ c_{yz} & c_{yy} & . & c_{zy} & c_{yy} & . \\ 0 & . & . & . & . & 0 \end{pmatrix}. \tag{26}$$

In Equation (16), excitation force vector $\boldsymbol{f}$ is a combined force from mass eccentricity excitation force vector $\boldsymbol{f}_m$, shaft bending excitation force vector $\boldsymbol{f}_r$ and magnet eccentricity force vector $\boldsymbol{f}_n$. The mass eccentricity excitation force vector is:

$$\boldsymbol{f}_m = \begin{pmatrix} 0 \\ \vdots \\ \hat{e}_m m_w \omega^2 \cos(\omega t + \varphi_m) \\ \hat{e}_m m_w \omega^2 \sin(\omega t + \varphi_m) \\ \vdots \\ 0 \end{pmatrix}_{12x1} \tag{27}$$

where is the rotor rotating speed and φ_m is the rotor rotating phase angle. Assuming that the radius of rotor is *R*, then, the bending moment *I* of rotor can be described as:

$$I = \frac{\pi R^4}{4}. \tag{28}$$

The following assumptions are made: the load which makes the rotor bend is uniformly distributed, the rotor distance between two sliding bearing is *L*, the rotor material modulus is *E*, then, the deflection of rotor can be expressed as:

$$\boldsymbol{e}_r = \frac{5\boldsymbol{f}_r L^3}{384EI}. \tag{29}$$

Based on Equation (29), $\boldsymbol{f}_r$ can be calculated as:

$$\boldsymbol{f}_r = \frac{384EI\boldsymbol{e}_r}{5L^3} = \frac{96E\pi R^4 \boldsymbol{e}_r}{5L^3}. \tag{30}$$

where $\boldsymbol{e}_r$ is the rotor shaft bending displacement vector and *L* is the rotor length between two sliding bearing. This force only acts on the rotor and sliding bearing film. The bending excitation force vector is:

$$\boldsymbol{f}_r = \begin{pmatrix} 0 \\ \vdots \\ \hat{e}_r \dfrac{96E\pi R^4}{5L^3} \cos(\omega t + \varphi_r) \\ \hat{e}_r \dfrac{96E\pi R^4}{5L^3} \sin(\omega t + \varphi_r) \\ 0 \\ -\hat{e}_r \dfrac{48E\pi R^4}{5L^3} \cos(\omega t + \varphi_r) \\ -\hat{e}_r \dfrac{48E\pi R^4}{5L^3} \sin(\omega t + \varphi_r) \\ \vdots \\ 0 \end{pmatrix}_{12x1}. \tag{31}$$

Magnet eccentricity forces are also referred as Unbalanced Magnetic Pulls (UMPs) force. The intensive studies on the causes of UMPs and the methods of calculating UMPs can be found in [1] [2] [3] [4] [5]. There are two types of

UMPs: static UMP and dynamic UMP. If the rotor center is offset from the stator center and it does not rotate around the stator center, the static UMP will be generated. UMP excitation force vector [11] is:

$$\boldsymbol{f}_{sn}=\begin{pmatrix} P_{AE\_Y}(\alpha)\times L_0 \\ P_{AE\_Z}(\alpha)\times L_0 \\ 0 \\ -P_{AE\_Y}(\alpha)\times L_0 \\ -P_{AE\_Z}(\alpha)\times L_0 \\ \vdots \\ 0 \end{pmatrix}_{12\times 1}. \tag{32}$$

where L_0 is the rotor effective length and

$$\begin{aligned} P_{AE\_Y}(\alpha)=\frac{\varepsilon R_A\pi}{2\mu_0}\times\Bigg\{&\sum_m f_{A2n}\,l_{Am}\cdot\cos\left[2np\omega t-(\alpha-\delta)\right]\Big|_{2np=mZ+2} \\ &-\sum_m f_{A2n}l_{Am}\cdot\cos\left[2np\omega t+(\alpha-\delta)\right]\Big|_{2np=mZ-2} \\ &+\sum_m f_{A2n}l_{Am}\cdot\cos\left[2np\omega t-(\alpha-\delta)\right]\Big|_{2np=mZ} \\ &-\sum_m f_{A2n}l_{Am}\cdot\cos\left[2np\omega t+(\alpha-\delta)\right]\Big|_{2np=mZ}\Bigg\}. \end{aligned} \tag{33}$$

And

$$\begin{aligned} P_{AE\_Z}(\alpha)=\frac{\varepsilon R_A\pi}{2\mu_0}\times\Bigg\{&\sum_m f_{A2n}\,l_{Am}\cdot\sin\left[2np\omega t-(\alpha-\delta)\right]\Big|_{2np=mZ+2} \\ &-\sum_m f_{A2n}l_{Am}\cdot\sin\left[2np\omega t+(\alpha-\delta)\right]\Big|_{2np=mZ-2} \\ &+\sum_m f_{A2n}l_{Am}\cdot\sin\left[2np\omega t-(\alpha-\delta)\right]\Big|_{2np=mZ} \\ &-\sum_m f_{A2n}l_{Am}\cdot\sin\left[2np\omega t+(\alpha-\delta)\right]\Big|_{2np=mZ}\Bigg\}. \end{aligned} \tag{34}$$

If the rotor center is offset from the stator center and it also rotates around the stator center, the dynamic UMP will be generated. The dynamic UMP excitation force vector is:

$$\boldsymbol{f}_{dn}=\begin{pmatrix} \frac{\varepsilon R_A L_0\pi}{2\mu_0} f_{A0}l_{A0}\cos\left[(2np+1)\omega t+\alpha\right] \\ \frac{\varepsilon R_A L_0\pi}{2\mu_0} f_{A0}l_{A0}\sin\left[(2np+1)\omega t+\alpha\right] \\ 0 \\ -\frac{\varepsilon R_A L_0\pi}{2\mu_0} f_{A0}l_{A0}\cos\left[(2np+1)\omega t+\alpha\right] \\ -\frac{\varepsilon R_A L_0\pi}{2\mu_0} f_{A0}l_{A0}\sin\left[(2np+1)\omega t+\alpha\right] \\ \vdots \\ 0 \end{pmatrix}_{12\times 1} \tag{35}$$

Regarding forced vibration, the standard harmonic excitation is considered,

and the equation of motion in frequency domain takes the form,

$$\left(-\omega^2 M + j\omega D + K\right)\{Q\} = \{F\} \tag{36}$$

where ω is the forcing frequency, $\{F\}$ is the complex force vector, and $\{Q\}$ is the complex response vector. For a given system having the properties ***M***, ***D***, ***C*** matrices and different type of exciting force $\{F\}$, the different complex response $\{Q\}$ can be obtained in frequency domain.

In order to identify the faults, we analyze the dynamic response of the proposed model excited by static and dynamic eccentricity forces. According to Laplace transform, the vibration response of static UMP in *y* and *z* direction can be expressed as;

$$\begin{aligned} y(t) = {} & \frac{P_0}{M\omega_n^2}\left\{1 - \frac{\mathrm{e}^{-\xi\omega_n t}}{\sqrt{1-\xi^2}}\sin\left[\omega_n\sqrt{1-\xi^2}\,t + \phi_1\right]\right\} \\ & + \frac{\varepsilon R_A \pi L_0}{2\mu_0 m} \times \sum_m f_{A2n} l_{Am} \cdot \frac{1}{4n^2p^2\omega^2\left(4n^2p^2\omega^2 + 4\xi\omega_n p\omega + \omega_n^2\right)}\cos\left(2np\omega t + \phi_m\right). \end{aligned} \tag{37}$$

And

$$z(t) = \frac{\varepsilon R_A \pi L_0}{2\mu_0 M} \times \sum_m f_{A2n} l_{Am} \cdot \frac{1}{4n^2p^2\omega^2\left(4n^2p^2\omega^2 + 4\xi\omega_n p\omega + \omega_n^2\right)}\sin\left(2np\omega t + \phi_m\right). \tag{38}$$

Using the same procedure, the vibration response of Dynamic UMP in *x* and *y* direction can be obtained as;

$$\begin{aligned} y(t) = {} & \frac{\varepsilon R_A \pi L_0}{2\mu_0 M} \times \left\{ f_1 l_1 \frac{1}{\omega^2\left(\omega^2 + 2\xi\omega_n\omega + \omega_n^2\right)}\cos\left(\omega t + \varphi_1\right)\right. \\ & \left. + \sum_m f_{A2n} l_{Am} \cdot \frac{1}{4n^2p^2\omega^2\left(4n^2p^2\omega^2 + 4\xi\omega_n p\omega + \omega_n^2\right)}\cos\left[\left(2np+1\right)\omega t + \varphi_m\right]\right\}. \end{aligned} \tag{39}$$

And

$$\begin{aligned} z(t) = {} & \frac{\varepsilon R_A \pi L_0}{2\mu_0 M} \times \left\{ f_1 l_1 \frac{1}{\omega^2\left(\omega^2 + 2\xi\omega_n\omega + \omega_n^2\right)}\sin\left(\omega t + \varphi_1\right)\right. \\ & \left. + \sum_m f_{A2n} l_{Am} \cdot \frac{1}{4n^2p^2\omega^2\left(4n^2p^2\omega^2 + 4\xi\omega_n p\omega + \omega_n^2\right)}\sin\left[\left(2np+1\right)\omega t + \varphi_m\right]\right\}. \end{aligned} \tag{40}$$

where p is the pole-pair number, φ_1 and φ_m are phase angle in first and m_{th} component respectively. Based on the equations from (37) to (40), we can make a conclusion in Table 1.

Table 1. Fault frequencies in static and dynamic eccentricities.

Fault type	y(Hz)			z (Hz)		
	$\omega/2\pi$	$2p\omega/2\pi$	$(2p+1)\omega/2\pi$	$\omega/2\pi$	$2p\omega/2\pi$	$(2p+1)\omega/2\pi$
Static eccentricity	No	**Yes**	No	No	**Yes**	No
Dynamic eccentricity	**Yes**	no	**Yes**	**Yes**	no	**Yes**

Table 1 shows that only number of pole order vibration has in the static eccentricity faulty motor. There are first order and number of pole plus one order vibration in the dynamic eccentricity faulty motor. These analytical results will be verification through experimental results later.

3. Results and Discussions

The experimental specimen design and vibration measurement are the same as in [11]. The real time vibration results of the healthy motor and the faulty ones with the static and dynamic eccentricities are shown in Figures 5(a)-(c) respectively. It can be seen that the faulty condition is difficult to be identified in time domain even though the low pass filter is used.

The rotor *y-z* orbits of the healthy motor, the faulty motor with static eccentricity, and that with the dynamic eccentricity are shown in Figures 6(a)-(c) respectively. It can be observed that the faulty motor and the healthy one can be easily differentiated; the vibration pattern of the healthy motor is much more regular than that of faulty motor. Moreover, the vibration amplitude of the healthy motor is much smaller than that of the faulty motor. Therefore, the technology can be adopted to distinguish faulty motor from healthy motor.

However, the type of fault cannot be distinguished, whether it is due to static or dynamic eccentricity. So the orbit of the rotor cannot be used as a tool to diagnose the motor running fault condition. Therefore, in this work, FFT signal processing algorithm is developed to obtain the vibration amplitude with different faulty grades and the results in each frequency in normalized percentage are shown in Table 2.

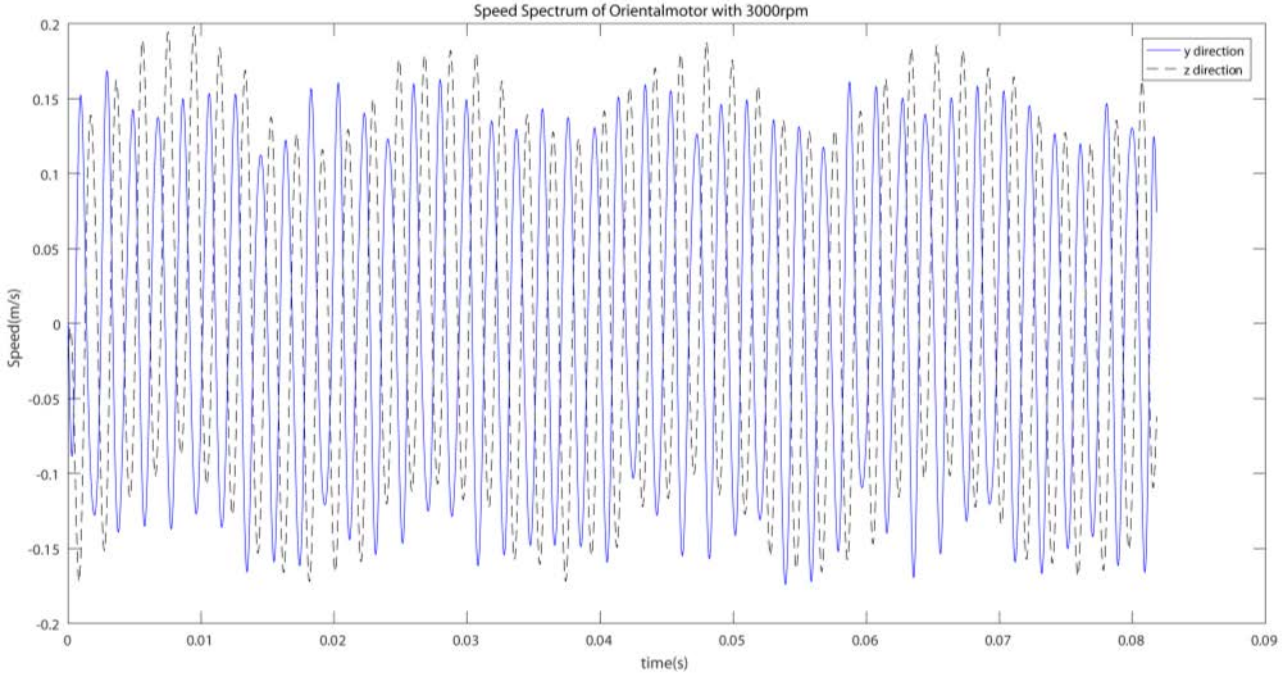

(a)

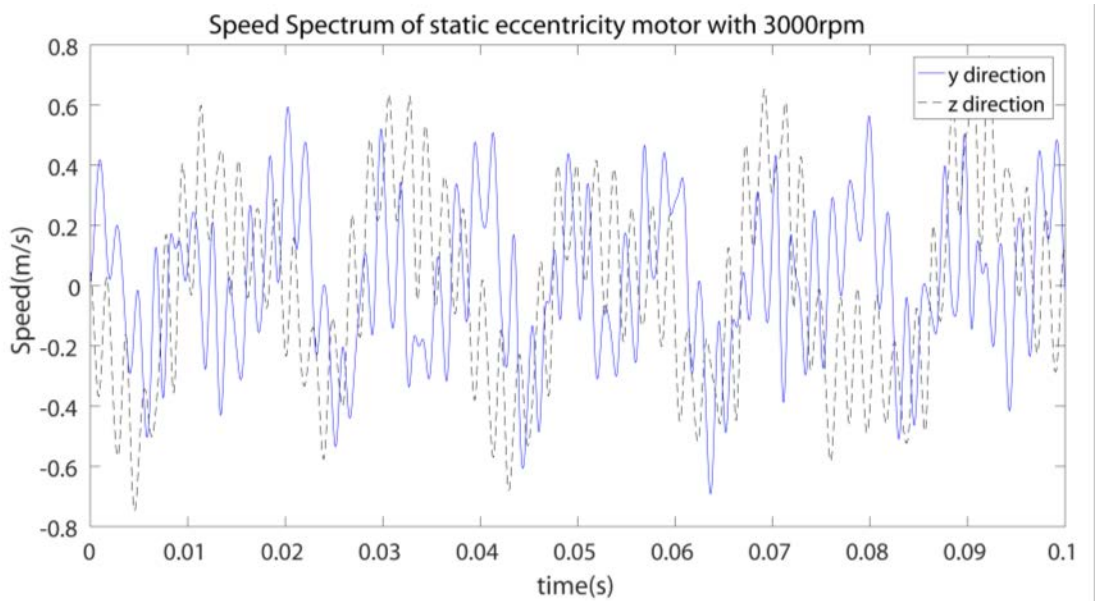

(b)

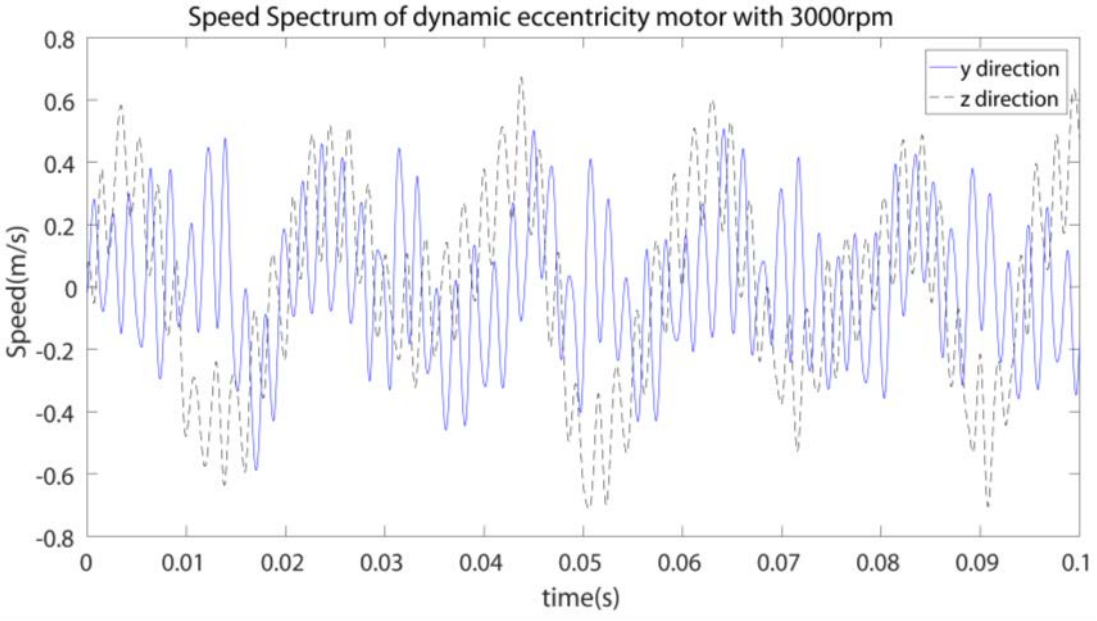

(c)

Figure 5. (a) Rotor vibration time spectrum of a healthy motor in radial direction. (b) Rotor vibration time spectrum of the faulty motor with static eccentricity in radial direction. (c) Rotor vibration time spectrum of the faulty motor with dynamic eccentricity in radial direction.

From the Table 2, we find that the vibration speed amplitude changes of static eccentricity is the largest in 10th orders of the running speed compared to others types of motor in two directions, we therefore can decide that the motor has a static eccentricity. On the other hand, we find that the vibration speed amplitude changes of dynamic eccentricity is the largest in 11th orders running speed compared to others types of motor in two directions. Moreover, there are second significant changes in 1st order running speed in the case of dynamic eccentricity.

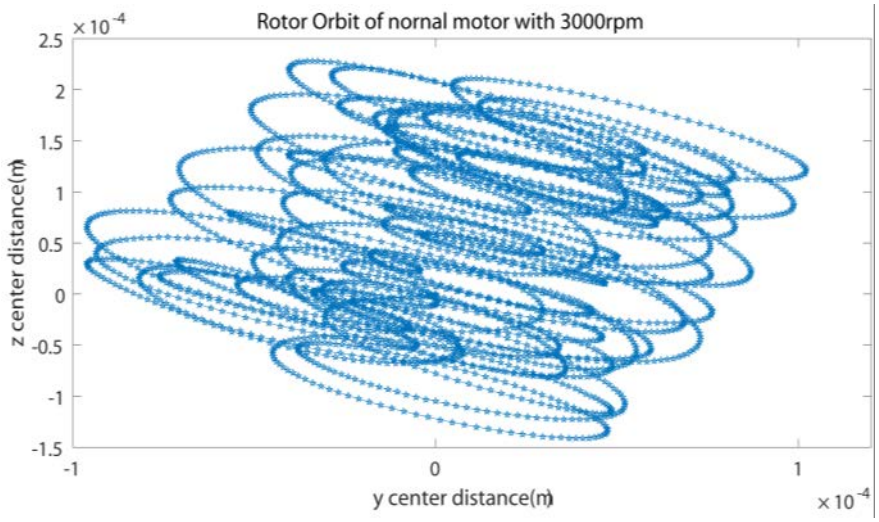

(a)

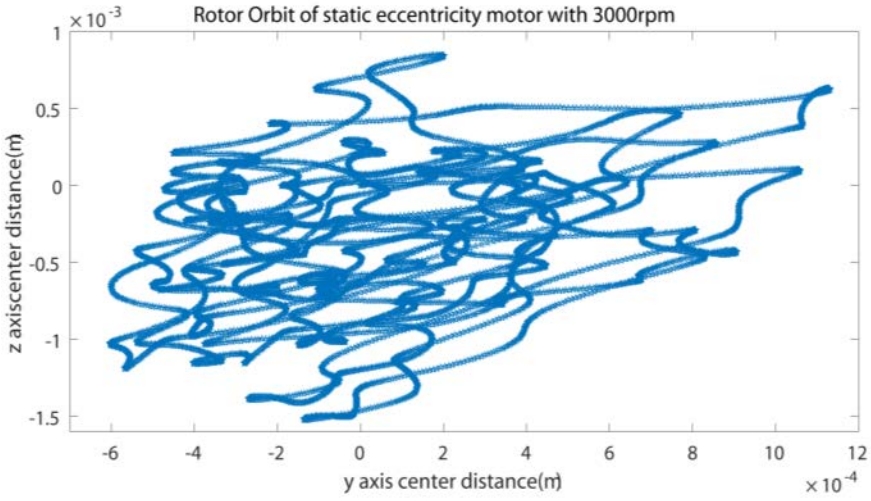

(b)

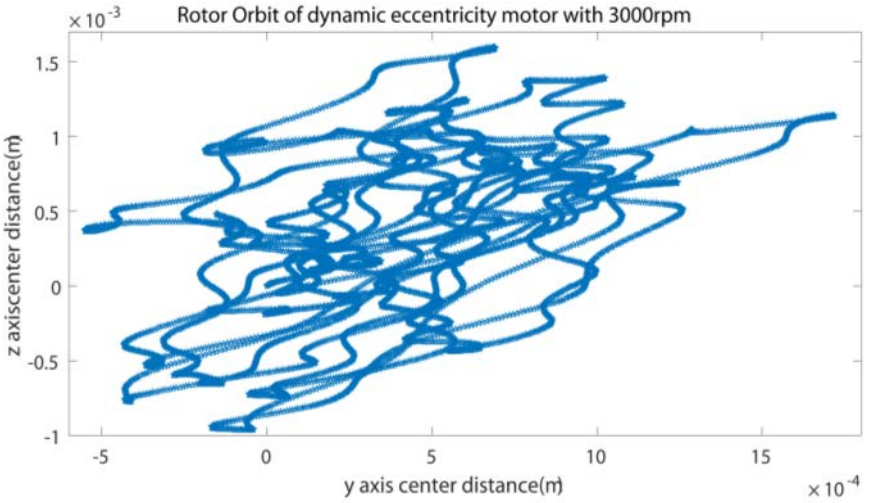

(c)

Figure 6. (a) Rotor x-y orbits of a healthy motor in radial direction. (b) Rotor x-y orbits of the faulty motor with static eccentricity in radial direction. (c) Rotor x-y orbits of the faulty motor with dynamic eccentricity in radial direction.

Table 2. Modulated FFT amplitude in difference faulty condition.

Fault grades	y(m/s)			z(m/s)		
No fault	50 Hz	500 Hz	550 Hz	50 Hz	500 Hz	550 Hz
	0.028978	0.161224	0.022174	0.034774	0.193543	0.026484
(a) SE results with different fault grades						
e1	0.04%	**0.27%**	0.17%	0.07%	**0.41%**	0.08%
e2	0.10%	**0.57%**	0.14%	0.08%	**0.88%**	0.17%
e3	0.08%	**0.87%**	0.17%	0.10%	**1.50%**	0.09%
e4	0.08%	**1.24%**	0.16%	0.09%	**2.49%**	0.09%
(b) DE results with different fault grades						
e1	**5.29%**	0.04%	**6.89%**	**6.69%**	2.31%	**12.23%**
e2	**9.31%**	0.04%	**12.14%**	**10.24%**	3.92%	**24.04%**
e3	**13.92%**	0.04%	**18.17%**	**14.16%**	5.63%	**36.50%**
e4	**18.98%**	0.04%	**24.78%**	**28.34%**	7.51%	**50.24%**

4. Conclusion

In this paper, we have introduced a mathematical model which takes into account the effects of three kinds of rotor eccentricities on the rotor dynamical response. An accurate dynamical response related to a magnetic-mechanical interaction in Permanent Magnet Synchronous Motors (PMSM) can be estimated using the model proposed in the paper. The forces due to rotor bending, rotor mass eccentricity and Unbalance Magnetic Pull (UMP) are calculated by considering the actual orbit of the rotor center and the actual orbit of the sliding bearing center. Based on the analytical results, we know that there is only pole number of faulty frequency signal can be observed if the motor has static eccentricity fault. On the other hand, there should be two faulty frequency signals in the observed faulty motor if the motor has dynamic eccentricity fault. The frequencies in the dynamic eccentricity motor are fundamental frequency and pole number plus one frequency. By using the filtered vibration signals alone in FFT domain, the healthy motor and different types of magnetic faulty motors can be distinguished successfully. In future, other types of motor fault can be studied through same procedure. Finally, the online monitoring system of the PMSM or other types of motor can be further developed. The developed system can be utilized in very critical application environment such as aerospace or smart renewable energy system.

References

[1] Salon, S.J. (1990) Finite Element Analysis of Electric Machinery. *IEEE Computer Applications in Power*, **3**, 29-32. https://doi.org/10.1109/67.53227

[2] Rajagopalan, S., Restrepo, J.A., Aller, J.M., Habetler, T.G. and Harley, R.G. (2005) Wigner-Ville Distributions for Detection of Rotor Faults in Brushless DC (BLDC) Motors Operating under Non-Stationary Conditions. 2005 5*th IEEE International Symposium on Diagnostics for Electric Machines, Power Electronics and Drives*, Vienna, Austria, 2005, 1-7. https://doi.org/10.1109/DEMPED.2005.4662511

[3] Huang, D.G. (2007) Characteristics of Torsional Vibrations of a Shaft with Unbalance. *Journal of Sound and Vibration*, **308**, 692-698. https://doi.org/10.1016/j.jsv.2007.04.005

[4] Concari, C., Tassoni, C. and Toscani, A. (2010) A New Method to Discern Mechanical Unbalances from Rotor Faults in Induction Machines. *XIX International Conference on Electrical Machines* (ICEM 2010), Rome, 4-8 September 2010, 2669-2676.

[5] Kr. Jalan, A. and Mohanty, A.R. (2009) Model Based Fault Diagnosis of a Rotor-Bearing System for Misalignment and Unbalance under Steady-State Condition. Journal of Sound and Vibration, **327**, 604-622. https://doi.org/10.1016/j.jsv.2009.07.014

[6] http://mathworld.wolfram.com/FastFourierTransform.html

[7] Garrigan, N.R., Soong, W.L., Stephens, C.M., Storace, A. and Lipo, T.A. (1999) Radial Force Characteristics of a Switched Reluctance Machine. *Industry Applications Conference*, 34*th IAS Annual Meeting*, October 3-7, 2250-2258. https://doi.org/10.1109/ias.1999.799158

[8] Werner, U. (2010) Theoretical Analysis of Shaft Vibrations in Two-Pole Induction Machines Considering Static Rotor Eccentricity. *SPEEDAM* 2010 *International Symposium on Power Electronics*, *Electrical Drives*, *Automation and Motion*, Pisa, 14-16 June 2010, 853-860. https://doi.org/10.1109/SPEEDAM.2010.5544902

[9] Rajagopalan, S., Aller, J.M., Restrepo, J.A., Habetler, T.G. and Harley, R.G. (2006) Detection of Rotor Faults in Brushless DC Motors Operating under Nonstationary Conditions. *IEEE Transactions on Industry Applications*, **42**, 1464–1477. https://doi.org/10.1109/TIA.2006.882613

[10] Bi, C., Aung, N.L.H., Soh, C.S., Jiang, Q., Phyu, H.N., Yu, Y.Q. and Lin, S. (2013) Influence of Neutral Line to the Optimal Drive Current of PMAC Motors. *IEEE Transactions on Magnetics*, **49**, 2483-2488. https://doi.org/10.1109/TMAG.2013.2245877

[11] Yu, Y.Q. (2014) Fault Diagnosis Permanent Magnet Synchronous Motor Based on Mechanical and Magnetic Characteristic Analysis. PhD Thesis.